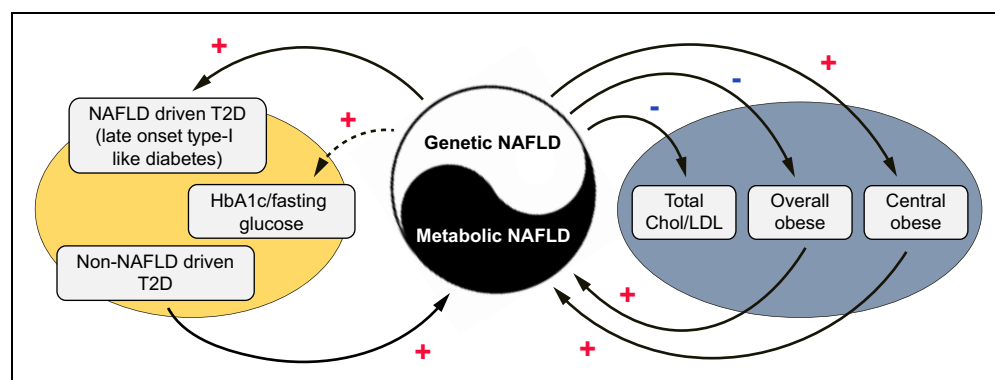


# Causal relationships between NAFLD, T2D and obesity have implications for disease subphenotyping

## Graphical abstract



## Authors

Zhipeng Liu, Yang Zhang,  
Sarah Graham, ..., Y.  
Eugene Chen,  
Cristen Willer,  
Wanqing Liu

## Correspondence

wliu@wayne.edu  
(W. Liu).

## Lay summary

Non-alcoholic fatty liver disease, type 2 diabetes and obesity are epidemiologically correlated with each other, but their causal relationships were incompletely understood. Herein, we identified causal relationships between these conditions, which suggest that each of these closely related diseases should be further stratified into subtypes. This is important for accurate diagnosis, prevention and treatment of these diseases.

## Highlights

- Genetic NAFLD promotes late onset type 1-like diabetes and central obesity but protects against overall obesity.
- Genetic NAFLD leads to lower circulating cholesterol.
- Genetically driven T2D and obesity causally increase the risk of NAFLD.
- PNPLA3-148M-driven NAFLD impairs insulin secretion but not insulin resistance.
- PNPLA3-148M-driven NAFLD activates thermogenesis pathway in peripheral fat tissue.



# Causal relationships between NAFLD, T2D and obesity have implications for disease subphenotyping

Zhipeng Liu<sup>1,#</sup>, Yang Zhang<sup>2,#</sup>, Sarah Graham<sup>3,#</sup>, Xiaokun Wang<sup>2</sup>, Defeng Cai<sup>2,4</sup>, Menghao Huang<sup>5</sup>, Roger Pique-Regi<sup>6</sup>, Xiaocheng Charlie Dong<sup>5</sup>, Y. Eugene Chen<sup>3</sup>, Cristen Willer<sup>3,7,8</sup>, Wanqing Liu<sup>1,2,9,\*</sup>

<sup>1</sup>Department of Medicinal Chemistry and Molecular Pharmacology, College of Pharmacy, Purdue University, West Lafayette, IN 47907, USA;

<sup>2</sup>Department of Pharmaceutical Sciences, Eugene Applebaum College of Pharmacy and Health Sciences, Wayne State University, Detroit, MI 48201, USA; <sup>3</sup>Department of Internal Medicine: Cardiology, University of Michigan, Ann Arbor, MI 48109, USA; <sup>4</sup>The Affiliated Shenzhen

Children's Hospital Laboratory Medicine, Shenzhen Children's Hospital, Shenzhen, 518038, China; <sup>5</sup>Department of Biochemistry and Molecular Biology, Indiana University School of Medicine, Indianapolis, IN 46202, USA; <sup>6</sup>Center for Molecular Medicine and Medical Genetics, School of Medicine, Wayne State University, Detroit, MI 48201, USA; <sup>7</sup>Department of Computational Medicine and Bioinformatics, University

of Michigan, Ann Arbor, MI 48109, USA; <sup>8</sup>Department of Human Genetics, University of Michigan, Ann Arbor, MI 48109, USA; <sup>9</sup>Department of Pharmacology, School of Medicine, Wayne State University, Detroit, MI 48201, USA

**Background & Aims:** Non-alcoholic fatty liver disease (NAFLD), type 2 diabetes (T2D) and obesity are epidemiologically correlated with each other but the causal inter-relationships between them remain incompletely understood. We aimed to explore the causal relationships between the 3 diseases.

**Methods:** Using both UK Biobank and publicly available genome-wide association study data, we performed a 2-sample bidirectional Mendelian randomization analysis to test the causal inter-relationships between NAFLD, T2D, and obesity. Transgenic mice expressing the human PNPLA3-I148M isoforms (TghPNPLA3-I148M) were used as an example to validate causal effects and explore underlying mechanisms.

**Results:** Genetically driven NAFLD significantly increased the risk of T2D and central obesity but not insulin resistance or generalized obesity, while genetically driven T2D, body mass index and WHRadjBMI causally increased NAFLD risk. The animal study focusing on PNPLA3 corroborated these causal effects: compared to the TghPNPLA3-I148I controls, the TghPNPLA3-I148M mice developed glucose intolerance and increased visceral fat, but maintained normal insulin sensitivity, reduced body weight, and decreased circulating total cholesterol. Mechanistically, the TghPNPLA3-I148M mice demonstrated decreased pancreatic insulin but increased glucagon secretion, which was associated with increased pancreatic inflammation. In addition, transcription of hepatic cholesterol biosynthesis pathway genes was significantly suppressed, while transcription of thermogenic pathway genes was activated in subcutaneous and brown adipose tissues but not in visceral fat in TghPNPLA3-I148M mice.

**Conclusions:** Our study suggests that lifelong, genetically driven NAFLD causally promotes T2D with a late-onset type 1-like diabetic subphenotype and central obesity; while genetically driven T2D, obesity, and central obesity all causally increase the risk of NAFLD. This causal relationship revealed new insights into how nature and nurture drive these diseases, providing novel hypotheses for disease subphenotyping.

**Lay summary:** Non-alcoholic fatty liver disease, type 2 diabetes and obesity are epidemiologically correlated with each other, but their causal relationships were incompletely understood. Herein, we identified causal relationships between these conditions, which suggest that each of these closely related diseases should be further stratified into subtypes. This is important for accurate diagnosis, prevention and treatment of these diseases.

© 2020 European Association for the Study of the Liver. Published by Elsevier B.V. All rights reserved.

## Introduction

Non-alcoholic fatty liver disease (NAFLD) is characterized by the presence of excess hepatic fat accumulation ( $\geq 5\%$ ) without significant alcohol use, hepatitis virus infection, or other secondary causes of hepatic fat accumulation.<sup>1</sup> The spectrum of NAFLD ranges from simple non-alcoholic fatty liver (NAFL) to non-alcoholic steatohepatitis (NASH), which over time can lead to cirrhosis, hepatocellular carcinoma, and organ failure.<sup>2</sup> Compelling observational epidemiological studies have shown that NAFLD is highly correlated with metabolic disorders such as type 2 diabetes (T2D)<sup>3–5</sup> and obesity.<sup>6,7</sup>

Dissecting the causal relationship between the 3 diseases is crucial for both understanding the disease etiology and developing effective diagnostic, therapeutic and preventive strategies. However, observational associations are limited in elucidating the causality due to various confounding factors (e.g. lifestyle, socioeconomic status) or the reverse causation bias.<sup>8</sup> As a result, the 3 diseases are often treated as comorbidities for each other in various biomedical research settings. Without clearly knowing the causality among the 3 diseases, treatments or preventive interventions may often lead to

**Keywords:** Mendelian randomization; Non-alcoholic fatty liver disease; Type 2 diabetes; Obesity; PNPLA3.

Received 21 August 2019; received in revised form 18 February 2020; accepted 3 March 2020; available online 10 March 2020

\* Corresponding author. Address: Department of Pharmaceutical Sciences, Eugene Applebaum College of Pharmacy and Health Sciences; and Department of Pharmacology, School of Medicine, Wayne State University, Detroit, MI 48201, USA; Integrative Biosciences Center Room 2401, 6135 Woodward Ave, Detroit, MI 48202, USA. Tel: 313-577-3375.

E-mail address: [wliu@wayne.edu](mailto:wliu@wayne.edu) (W. Liu).

# Equal contribution.

<https://doi.org/10.1016/j.jhep.2020.03.006>



ELSEVIER

conflicting research findings and inconsistent responses among patients.

Mendelian randomization (MR) analysis, which uses genetic variants as proxies for the risk factors of interest, has been widely applied in understanding the causal relationship between various risk factors and human diseases, e.g. estimation of the causal effect of plasma high-density lipoprotein (HDL) cholesterol on myocardial infarction risk.<sup>9</sup> Since during the process of meiosis the alleles of the parents are randomly segregated to the offspring, the MR method is considered to be analogous to a randomized controlled trial but less likely to be influenced by confounding factors and reverse causation.<sup>10</sup> Bidirectional MR is an extension of traditional MR in which the exposure-outcome causal relationship was explored from both sides. The bidirectional framework provides an efficient way to ascertain the direction of a causal relationship, which helps alleviate the potential bias from reverse causation.<sup>11</sup>

Recent MR studies have partially explored the causal relationships among the 3 diseases. Dongiovanni *et al.* showed that genetically driven hepatic steatosis was associated with insulin resistance and a small increase in T2D risk.<sup>12</sup> A study by De Silva *et al.* indicated that genetically elevated circulating alanine aminotransferase (ALT) and aspartate aminotransferase (AST) increased the risk of T2D.<sup>13</sup> Stender *et al.* found that the genetic predictors of body mass index (BMI) were associated with NAFLD.<sup>14</sup> However, a systematic bidirectional MR study leveraging the latest genome-wide association study (GWAS) data is needed to elucidate the causal relationships among the 3 diseases in a uniform setting. In addition, experimental analysis e.g. animal models with a characterized natural history under controlled conditions would also help further establish causality.

In this study, we first aimed to explore whether NAFLD causally increases the risk of T2D, obesity and their related intermediate traits. We then investigated the reverse relationships, i.e. whether T2D and obesity causally affect NAFLD risk. In addition, we used a newly constructed transgenic mice model expressing human PNPLA3-I148M isoforms, a known genetic NAFLD model, as a typical example to validate the causal effects of NAFLD on T2D and obesity identified in humans, as well as to explore the potential mechanisms underlying these causal relationships.

## Materials and methods

### Ethics statement

The summary-level GWAS data used for MR analyses are publicly available<sup>15–24</sup> (Fig. 1 and Table S1). Therefore, no specific ethical approval is required. The study of the transgenic mice experiments has been reviewed and approved by the IACUC of both Wayne State University and the Indiana University School of Medicine. This research has been conducted using the UK Biobank Resource under application number 24460.

### MR analyses

#### GWAS summary data

We extracted the significant variants ( $p < 5 \times 10^{-8}$ ) associated with hepatic steatosis and histologic NAFLD from the largest GWAS study to date.<sup>15</sup> For the purpose of estimating the reverse causal relationship, we generated the full GWAS summary statistics of NAFLD in UK Biobank (UKBB) samples consisting of 1,122 cases and 399,900 controls. The details of the GWAS of NAFLD in UKBB are described in the section below.

We downloaded full GWAS summary data of 22 glycemic and obesity traits from the largest published studies as of March 2019. Only association results from participants of European descent were used in the present study. The details on the phenotype information, sample size, and PubMed ID of the original study are summarized in Table S1.

#### GWAS of NAFLD and T2D in UK Biobank

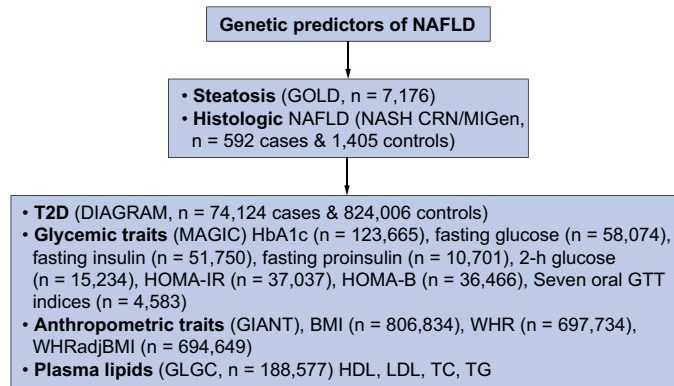
NAFLD was defined based on ICD-9 571.8 “Other chronic non-alcoholic liver disease”) and ICD-10 K76.0 [“Fatty (change of) liver, not elsewhere classified”) from inpatient hospital diagnosis within the UKBB dataset. Individuals with hepatitis B or C or with other known liver diseases (e.g. liver transplant, hepatomegaly, jaundice, or abnormal liver function study results) were excluded from the analysis. Notably, we recognized that this medical record-based phenotype may not exactly reflect the clinically/histologically characterized NAFLD. However, we found that the top genetic risk alleles identified in our GWAS matched the patterns of previously identified loci for NAFLD/NASH, suggesting that the phenotypic definition in the UKBB reflect that of clinical NAFLD very well. The white British subset of the UKBB was used for analysis in SAIGE<sup>25</sup> with sex, birth year, and 4 principle components as covariates.

#### Genetic predictors selection

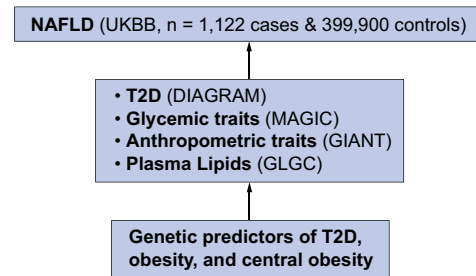
We used the 2 strongest genetic predictors of NAFLD, patatin-like phospholipase domain-containing protein 3 (PNPLA3) rs738409 and transmembrane 6 superfamily member 2 (TM6SF2) rs58542926, as the proxy for hepatic steatosis and histologic NAFLD. We chose these 2 variants as the instruments based on the following rationale: i) These 2 variants have been consistently shown to be associated with the whole spectrum of NAFLD.<sup>15,26–29</sup> Among numerous genetic association analyses, the association between these 2 variants and NAFLD and related traits are the most significant. Their associations with NAFLD are also much stronger than those with other traits. ii) Mechanistic studies have clearly demonstrated that these 2 variants are causal to NAFLD.<sup>27,30–32</sup> iii) Both genes are only highly expressed in limited tissues/organs, especially in the liver. According to the GTEx data, PNPLA3 is mainly expressed in the liver and skin/adipose tissue as opposed to other tissues, while TM6SF2 is almost exclusively expressed in the intestine and liver. iv) These 2 variants have been broadly accepted as genetic proxies to infer the causal relationship between NAFLD/liver fat/liver function enzyme and complex traits including liver damage and insulin resistance,<sup>12</sup> ischemic heart disease,<sup>33</sup> and vitamin D intake and deficiency.<sup>34</sup> As TM6SF2 rs58542926 is not genotyped in most of the GWAS summary data used in this study, rs2228603 at the NCAN gene locus, which is in strong linkage disequilibrium with TM6SF2 rs58542926 (pairwise  $R^2 = 0.76$  based on the phase 3 data of the 1000 Genomes Project in European individuals) and significantly associated with both hepatic fat content and NAFLD histology,<sup>35</sup> was used as the proxy for TM6SF2 rs58542926.

For the 22 glycemic and obesity traits, we selected the significant and independent genetic predictors in 2 steps: we first obtained all the variants that passed the genome-wide association significance level of  $p < 5 \times 10^{-8}$ . Then the independent genetic predictors were identified by clumping the top GWAS loci through PLINK 1.9 (<https://www.cog-genomics.org/plink2>) with the threshold of LD  $R^2 < 0.1$  in a 500 kb window. The linkage disequilibrium was estimated based on the European samples in

> Step 1: Whether NAFLD causally affects T2D, obesity and their related traits?



> Step 2: Whether T2D, obesity and their related traits causally affect NAFLD?



> Step 3: Whether the causal relationships between NAFLD and T2D and obesity can be replicated in animal model?

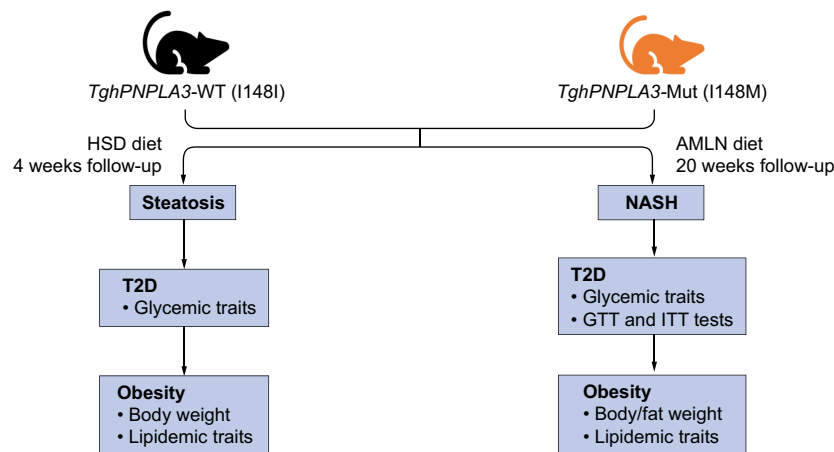


**Fig. 1. Flowchart of the study design.** The summary-level associations were taken from the following genomics consortium: GOLD for CT-measured hepatic steatosis<sup>15</sup>; NASH CRN and MIGen for biopsy-proven NAFLD<sup>15</sup>; DIAGRAM for T2D<sup>16</sup>; MAGIC consortium for glycemic traits including HbA1c,<sup>17</sup> fasting glucose,<sup>18</sup> fasting insulin,<sup>18</sup> fasting proinsulin,<sup>19</sup> 2-h glucose,<sup>20</sup> HOMA-IR<sup>21</sup> and HOMA-B,<sup>21</sup> and 7 insulin secretion and action indices during OGTT<sup>22</sup>; The GIANT consortium for BMI, WHR, and WHRadjBMI<sup>23</sup>; The GLGC for plasma HDL, LDL, TC, TG levels.<sup>24</sup> BMI, body mass index; GTT, glucose tolerance test; HbA1c, glycated hemoglobin; HDL, high-density lipoprotein cholesterol; HOMA-IR, homeostatic model assessment of insulin resistance; HOMA-B, homeostatic model assessment of  $\beta$ -cell function; ITT, insulin tolerance test; NAFLD, non-alcoholic fatty liver disease; NASH, non-alcoholic steatohepatitis; T2D, type 2 diabetes; TC, total cholesterol; TG, triglycerides; WHR, waist-hip ratio; WHRadjBMI, WHR adjusted for BMI; WT, wild-type. (This figure appears in color on the web.)

phase 3 of the 1000 Genomes Project.<sup>36</sup> We omitted 10 traits including 2 h glucose, homeostatic model assessment of insulin resistance (HOMA-IR), HOMA-B, and 7 oral glucose tolerance test (OGTT) traits due to lack of enough significant and independent genetic variants (number of valid variants <3). Therefore, 12 traits were analyzed for their causal effects on NAFLD. The F statistics of all the genetic predictors in the present study were larger than the empirical threshold of  $10^{37}$  (Table 1 and Table 2).

#### MR estimation

For MR estimation with NAFLD as the exposure, we used the inverse variance weighted (IVW) method to estimate the combined causal effect of *PNPLA3* and *TM6SF2* (*NCAN*) variants by assuming a fixed-effect model.<sup>38</sup> As a sensitivity analysis, Wald's method was used to estimate the causal effect for each genetic variant. We considered a significant causal relationship if the directions of the estimates by *PNPLA3*, *TM6SF2* (*NCAN*), and the 2

variants combined were consistent, and the combined estimate passed the Bonferroni-adjusted significance of  $p < 0.05$ .

For the MR estimation with NAFLD as the outcome, besides the IVW method, we estimated the causal effects using additional methods including weighted median estimator<sup>39</sup> and MR-Egger<sup>40</sup> as a sensitivity analysis. To assess the heterogeneity and identify horizontal pleiotropic outliers, we used the Q' statistics<sup>41</sup> with modified second order weights and MR-PRESSO global test.<sup>42</sup> If the horizontal pleiotropy is significant, MR-PRESSO was used to identify outliers at  $p < 0.05$ . We then removed the outliers and retested if the causal relationship and pleiotropic effects were significant. We considered the relationships significant if the directions of the estimates by 3 methods (IVW, weighted median, and MR-Egger) were consistent, the IVW method passed the Bonferroni-adjusted significance of  $p < 0.05$ , and there was no significant pleiotropy tested by MR-PRESSO global test and modified Q' statistics. MR analyses were performed with "MendelianRandomization",<sup>43</sup> "MRPRESSO",<sup>42</sup> and "RadialMR"<sup>44</sup> packages in R version 3.5.0 (<http://www.r-project.org/>).



**Table 1. MR estimates with hepatic steatosis or histologic NAFLD as the exposure.**

|                                      | Hepatic steatosis (per SD) |          | Histologic NAFLD (per logOR) |          |
|--------------------------------------|----------------------------|----------|------------------------------|----------|
|                                      | Effect (95% CI)            | p Value  | Effect (95% CI)              | p Value  |
| <b>T2D and glycemic traits</b>       |                            |          |                              |          |
| T2D (OR)                             | 1.30 (1.21 to 1.39)        | 8.30E-14 | 1.06 (1.03 to 1.09)          | 2.80E-04 |
| HbA1c (%)                            | -0.0072 (-0.025 to 0.01)   | 4.20E-01 | -0.0025 (-0.0074 to 0.0024)  | 3.10E-01 |
| Fasting glucose (mmol/L)             | 0.026 (8.5E-05 to 0.051)   | 4.90E-02 | 0.0032 (-0.0031 to 0.0096)   | 3.20E-01 |
| Fasting insulin (pmol/L)             | 0.025 (0.0035 to 0.046)    | 2.20E-02 | 0.0064 (0.00034 to 0.012)    | 3.80E-02 |
| Fasting proinsulin (pmol/L)          | 0.032 (-0.026 to 0.089)    | 2.80E-01 | 0.0051 (-0.0091 to 0.019)    | 4.80E-01 |
| 2h glucose (mmol/L)                  | -0.066 (-0.21 to 0.079)    | 3.70E-01 | -0.015 (-0.051 to 0.021)     | 4.10E-01 |
| HOMA-IR ((mU/L)*(mmol/L))            | 0.03 (-0.0016 to 0.061)    | 6.30E-02 | 0.0066 (-0.0016 to 0.015)    | 1.10E-01 |
| HOMA-B ((mU/L)/(mmol/L))             | 0.007 (-0.019 to 0.033)    | 5.90E-01 | 0.0011 (-0.0052 to 0.0074)   | 7.30E-01 |
| AUCins (mU*min/L)                    | -0.012 (-0.18 to 0.16)     | 8.90E-01 | -0.0043 (-0.046 to 0.038)    | 8.40E-01 |
| AUCins/AUCgluc (mU/mmol)             | -0.01 (-0.18 to 0.16)      | 9.10E-01 | -0.0037 (-0.046 to 0.038)    | 8.60E-01 |
| Incre30 (mU/L)                       | -0.0021 (-0.17 to 0.16)    | 9.80E-01 | -0.00033 (-0.041 to 0.04)    | 9.90E-01 |
| Ins30adjBMI                          | 0.017 (-0.15 to 0.19)      | 8.40E-01 | 0.00083 (-0.041 to 0.043)    | 9.70E-01 |
| ISI (mg/dl)                          | 0.011 (-0.18 to 0.2)       | 9.10E-01 | 0.017 (-0.032 to 0.065)      | 5.00E-01 |
| CIAdjBMI                             | -0.0055 (-0.18 to 0.17)    | 9.50E-01 | -0.0034 (-0.045 to 0.039)    | 8.80E-01 |
| DI                                   | 0.078 (-0.082 to 0.24)     | 3.40E-01 | 0.022 (-0.018 to 0.063)      | 2.80E-01 |
| <b>Obesity and lipid traits (SD)</b> |                            |          |                              |          |
| BMI                                  | -0.027 (-0.041 to -0.013)  | 1.30E-04 | -0.0071 (-0.012 to -0.0023)  | 3.40E-03 |
| WHR                                  | 0.021 (0.0062 to 0.036)    | 5.40E-03 | 0.0029 (-0.00091 to 0.0067)  | 1.30E-01 |
| WHRadjBMI                            | 0.039 (0.023 to 0.054)     | 8.20E-07 | 0.0072 (0.0022 to 0.012)     | 4.50E-03 |
| HDL-c                                | -0.028 (-0.062 to 0.0071)  | 1.20E-01 | -0.0096 (-0.021 to 0.0013)   | 8.30E-02 |
| LDL-c                                | -0.098 (-0.14 to -0.053)   | 2.30E-05 | -0.014 (-0.026 to -0.0012)   | 3.10E-02 |
| TC                                   | -0.12 (-0.17 to -0.074)    | 3.30E-07 | -0.019 (-0.033 to -0.0054)   | 6.80E-03 |
| TG                                   | -0.02 (-0.06 to 0.021)     | 3.40E-01 | 0.0038 (-0.0057 to 0.013)    | 4.40E-01 |

Effect was estimated by a combined genetic vector of *PNPLA3* and *TM6SF2* (*NCAN*) variants through IVW method. The F statistics of the genetic predictors of hepatic steatosis and histologic NAFLD are 110 and 10, respectively. *p* values less than Bonferroni-adjusted level of significance ( $p < 0.05/20 = 2.5E-03$ ) were considered as significant. AUCins, AUC of insulin levels during oral glucose tolerance test (OGTT); AUCins/AUCgluc, ratio of AUC insulin and AUC glucose; BMI, body mass index; CIAdjBMI, corrected insulin response adjusted for ISI; DI, disposition index; HbA1c, glycated hemoglobin; HDL-c, high-density lipoprotein cholesterol; HOMA-B, homeostatic model assessment of beta cell function; HOMA-IR, homeostatic model assessment of insulin resistance; Ins30adjBMI, insulin response to glucose during the first 30 min adjusted for BMI; Incre30, incremental insulin at 30 min; ISI, insulin sensitivity index; IVW, inverse variance weighted; LDL-c, low-density lipoprotein cholesterol; OR, odds ratio; T2D, type 2 diabetes; TC, total cholesterol; TGs, triglycerides; WHR, waist-hip ratio; WHRadjBMI, WHR adjusted for BMI.

### Sensitivity analysis

To test the robustness of the MR estimation, we incorporated more known but less significant GWAS-identified NAFLD risk variants as the genetic proxy. The sensitivity analysis was performed using summary data from 2 independent NAFLD GWASs. Firstly, we re-estimated the causal effects of hepatic steatosis and histologic NAFLD on T2D, obesity, and their related traits using all 5 NAFLD risk variants (*PNPLA3* rs738409, *NCAN* rs2228603, *GCKR* rs780094, *PPP1R3B* rs4240624, and *LYPLAL1* rs12137855) identified in the GOLD (Genetics of Obesity-related Liver Disease) cohort. Next, to incorporate 2 other known NAFLD risk variants (*MBOAT-TM4* rs641738 and *HSD17B13* rs6834314), we extracted the summary statistics of all 7 known variants from the UKBB NAFLD GWAS summary data. The MR estimation was performed using different combinations of the variants through the IVW method.

### Animal experiments

We constructed transgenic mouse model expressing human *PNPLA3*-I148I and *PNPLA3*-I148M isoforms, respectively. The mice were either fed with a high-sucrose diet (HSD)<sup>31</sup> for 4 weeks to induce hepatosteatosis, or a high-fat, high-fructose and high-cholesterol diet (known as the Amylin or AMLN diet)<sup>45–48</sup> for 20 weeks to induce NASH. T2D and obesity phenotypes were characterized during the dietary feeding. Various experimental analyses were performed to explore the mechanism underlying the causal relationships between NAFLD, T2D and obesity, including: histologic analyses of the mouse liver tissue; immunofluorescent staining of inflammation makers in both

liver and pancreas tissue, as well as the insulin and glucagon signaling in pancreas tissue; western blot analysis of Akt signaling in the liver and skeletal muscle tissues; real-time PCR to examine the gene expression levels of hepatic cholesterol biosynthesis and thermogenesis pathway genes in brown and white (subcutaneous and epididymal) adipose tissues. Details on the transgenic mouse model construction and technical methods and materials for various phenotypic characterization and molecular assays are described in the [supplementary information](#).

### Statistical analyses

Power assessments for the animal study are described in the [supplementary methods](#). Statistical significance assessments were performed using ANOVA, Student's *t* test or Pearson correlation wherever appropriate. Tukey corrected *p* values <0.05 were considered significant. All statistical analyses for animal experiments were performed using GraphPad Prism Version 6.00 (GraphPad Software, CA, USA).

For further details regarding the materials and methods used, please refer to the [CTAT table](#) and [supplementary information](#).

## Results

### Study overview

The design of this study consists of 3 steps ([Fig. 1](#)). We first aimed to explore whether NAFLD (both CT-measured hepatic steatosis and biopsy-proven histologic NAFLD) causally affects T2D, obesity and their related intermediate traits (Step 1). To this end, we used the summary GWAS data for CT scan-measured steatosis (GOLD) as well as the histologic NAFLD (case and control) (NASH

Table 2. MR estimate with NAFLD as the outcome.

|                                       | #SNPs | F   | IVW                 |          | Weighted median     |          | MR-Egger                |          | Pleiotropy test                    |          |
|---------------------------------------|-------|-----|---------------------|----------|---------------------|----------|-------------------------|----------|------------------------------------|----------|
|                                       |       |     | OR (95% CI)         | p value  | OR (95% CI)         | p value  | OR (95% CI)             | p value  | modified Q <sup>a</sup><br>p value |          |
| T2D and glycemic traits <sup>#</sup>  |       |     |                     |          |                     |          |                         |          |                                    |          |
| T2D (logOR) <sup>*</sup>              | 315   | 69  | 1.1 (1 to 1.2)      | 1.67E-03 | 1.1 (0.93 to 1.2)   | 3.54E-01 | 0.99 (0.84 to 1.2)      | 8.59E-01 | 3.11E-01                           | 3.26E-01 |
| HbA1c (%)                             | 67    | 69  | 0.33 (0.17 to 0.66) | 1.76E-03 | 0.33 (0.11 to 1.11) | 7.44E-02 | 0.17 (0.04 to 0.68)     | 1.28E-02 | 3.85E-01                           | 3.69E-01 |
| Fasting glucose (mmol/L)              | 33    | 68  | 0.42 (0.25 to 0.73) | 1.60E-03 | 0.33 (0.15 to 0.80) | 1.34E-02 | 0.44 (0.12 to 1.52)     | 1.93E-01 | 8.78E-02                           | 8.29E-02 |
| Fasting insulin (pmol/L) <sup>*</sup> | 9     | 36  | 7.7 (1.3 to 46)     | 2.40E-02 | 4.6 (0.42 to 51)    | 2.11E-01 | 4.2 (0.00035 to 51,000) | 7.64E-01 | 3.18E-01                           | 2.82E-01 |
| Fasting proinsulin (pmol/L)           | 15    | 72  | 1.13 (0.79 to 1.62) | 4.94E-01 | 0.99 (0.58 to 1.67) | 9.55E-01 | 1.57 (0.49 to 4.95)     | 4.51E-01 | 4.60E-02                           | 4.74E-02 |
| Obesity and lipid traits              |       |     |                     |          |                     |          |                         |          |                                    |          |
| BMI <sup>*</sup>                      | 1,839 | 60  | 2.3 (2 to 2.7)      | 1.41E-25 | 2.1 (1.6 to 2.8)    | 1.02E-07 | 1.7 (1.1 to 2.7)        | 1.58E-02 | 2.50E-03                           | 3.89E-03 |
| WHR                                   | 951   | 53  | 2.10 (1.72 to 2.59) | 2.85E-12 | 2.34 (1.67 to 3.32) | 6.91E-07 | 1.62 (0.94 to 2.72)     | 8.14E-02 | 3.62E-01                           | 3.64E-01 |
| WHRadjBMI                             | 1,156 | 63  | 1.54 (1.30 to 1.82) | 1.11E-06 | 1.60 (1.20 to 2.14) | 1.53E-03 | 1.57 (1.06 to 2.34)     | 2.37E-02 | 4.55E-01                           | 4.54E-01 |
| HDL-c <sup>*</sup>                    | 226   | 123 | 0.88 (0.76 to 1)    | 8.78E-02 | 0.83 (0.64 to 1.1)  | 1.57E-01 | 0.93 (0.69 to 1.3)      | 6.62E-01 | 2.00E-03                           | 1.26E-03 |
| LDL-c <sup>*</sup>                    | 192   | 148 | 0.96 (0.84 to 1.1)  | 5.47E-01 | 1 (0.79 to 1.3)     | 9.69E-01 | 0.84 (0.64 to 1.1)      | 2.11E-01 | <5.00E-04                          | 7.29E-06 |
| TC <sup>*</sup>                       | 239   | 110 | 0.94 (0.82 to 1.1)  | 4.18E-01 | 0.95 (0.71 to 1.3)  | 7.13E-01 | 0.88 (0.66 to 1.2)      | 3.85E-01 | 1.00E-03                           | 6.33E-04 |
| TG <sup>*</sup>                       | 149   | 119 | 1.6 (1.3 to 1.9)    | 5.10E-07 | 1.7 (1.2 to 2.4)    | 1.45E-03 | 1.7 (1.1 to 2.4)        | 8.92E-03 | 7.00E-03                           | 7.83E-03 |

We considered as significant if the directions of the estimates by IVW, median, Egger were consistent, IVW method passed the Bonferroni corrected threshold (0.05/12 = 4.2E-03), and no significant pleiotropy tested by MR-PRESSO global test and modified Q<sup>a</sup> statistics (both  $p > 0.05$ ).

<sup>a</sup>Outlier variants were identified and removed by MR-PRESSO at  $p < 0.05$ . Initial estimates without removing outliers were shown in Table S5.

<sup>b</sup>Ten traits including 2 h glucose, HOMA-IR, HOMA-B, and 7 OGTT traits were omitted due to lack of enough significant and independent genetic variants (number of valid variants <3). BMI, body mass index; F, F statistics for the strength of correlation between instrument and exposure; HOMA-B, homeostatic model assessment of beta cell function; HOMA-IR, homeostatic model assessment of insulin resistance; IVW, inverse variance weighted; MR-PRESSO, MR pleiotropy residual sum and outlier; OGTT, oral glucose tolerance test; OR, odds ratio; Q<sup>a</sup>, Q statistics with modified second order weights; SNPs, single nucleotide polymorphisms; T2D, type 2 diabetes; TC, total cholesterol; TG, triglycerides; WHR, waist-hip ratio; WHRadjBMI, WHR adjusted for BMI.

CRN/MIGen) presented in Speliotes *et al.*,<sup>15</sup> which is thus far the largest GWAS comprehensively covering multiple phenotypes of NAFLD. We also use the summary GWAS meta-analysis data for T2D (DIAGRAM),<sup>16</sup> obesity (GIANT),<sup>23</sup> glycemic (MAGIC)<sup>17–22</sup> and lipid (GLGC)<sup>24</sup> traits as outcomes (Step 1), which are the largest GWASs to date on these phenotypes. The causal role of NAFLD on T2D and obesity was assessed first by using 2 well-established NAFLD-associated polymorphisms in *PNPLA3* and *TM6SF2/NCAN* loci as proxies for hepatic steatosis and histologic NAFLD. We then performed a GWAS on the NAFLD phenotype in the UKBB dataset. Based on this new summary data, we further performed a sensitivity analysis by including 5 other GWAS-identified variants as a broad proxy for NAFLD to further examine the causal relationship between NAFLD and T2D or obesity. Second, using the aforementioned summary-level data of UKBB, DIAGRAM and GIANT, we then investigated the reverse relationships, i.e. whether T2D or obesity causally affect NAFLD risk in the UKBB samples (Step 2). Finally, we constructed a transgenic mouse model expressing human *PNPLA3-I148I* or *PNPLA3-I148M* isoforms. We aim to use this established typical genetic model for NAFLD as an example to further validate the causal effects of hepatic steatosis or NAFLD on T2D and obesity, as well as to explore the potential mechanisms underlying these causal effects (Step 3). To test the effect of steatosis and histologic NAFLD on the susceptibility to T2D and obesity, we used a HSD known to induce steatosis in *PNPLA3-I148M* mice,<sup>31</sup> as well as the Amylin or AMLN diet, which is known to induce NASH in mice.<sup>45–48</sup> A schematic representation of the 3 assumptions for an MR analysis was shown in Fig. S1A, and the MR methods and heterogeneity tests used in the study were listed in Fig. S1B.

### The causal effect of NAFLD on T2D risk and glycemic traits

We first used 2 well-established NAFLD-associated variants in *PNPLA3* (rs738409) and *TM6SF2/NCAN* (rs2228603) gene loci as the genetic instruments to test the causal effect of NAFLD on T2D and glycemic traits in the latest publicly available GWAS data. As listed in Table 1, we observed a significant association between genetically driven hepatic steatosis and T2D risk, in which a 1 SD increase in CT-measured hepatic steatosis caused a 30% increased risk of T2D (odds ratio [OR] 1.3; 95% CI 1.2–1.4;  $p = 8.3E-14$ ). As for glycemic traits, we detected nominal weak associations of steatosis with increased fasting glucose ( $\beta$  0.026 mmol/L; 95% CI 8.5E-05 to 0.051;  $p = 0.049$ ), fasting insulin ( $\beta$  0.025 pmol/L; 95% CI 0.0035–0.046;  $p = 0.022$ ). These results were not significant after adjusted with Bonferroni correction ( $p < 2.5E-03$ , correction for 20 traits except HOMA-IR and HOMA-B due to the collinearity with glucose and insulin levels). There was no causal relationship between genetically driven hepatic steatosis and insulin resistance (HOMA-IR) ( $\beta$  0.03 (mU/L) (mmol/L); 95% CI –0.0016 to 0.061;  $p = 0.063$ ) levels. Other tested glycemic traits including glycated hemoglobin (HbA1c), fasting proinsulin, 2-h glucose, HOMA-B, and 7 insulin secretion and action indices during OGTT did not show any significance either.

We then tested if a genetically increased risk of histologic NAFLD also has a causal effect on T2D susceptibility and glycemic traits. Consistent with the result of hepatic steatosis, there was evidence of a significant effect of histologically characterized NAFLD severity on an increased risk of T2D (OR 1.06; 95% CI 1.03–1.09;  $p = 2.8E-04$ ). Again, no significant causal relationship was found between genetically driven NAFLD and glycemic traits especially after adjusting for multiple testing (Table 1). Taken

together, genetically driven NAFLD causally increased the risk of T2D, but not insulin resistance or other glycemic traits.

### The causal impact of NAFLD on obesity

While obesity is a well-known risk factor for NAFLD, the reverse relationship, i.e. the causal effect of NAFLD on obesity, has not been explored before. Using the same genetic predictors of steatosis and histologic NAFLD, we implemented MR and observed a significant causal association of a 1 SD increase in hepatic fat with a 0.027 SD decrease in BMI ( $\beta$  -0.027; 95% CI -0.043 to -0.013;  $p$  = 1.3E-04), but a 0.039 SD increase in WHRadjBMI (WHR adjusted for BMI), an established marker for abdominal or central obesity ( $\beta$  0.039; 95% CI 0.023–0.054;  $p$  = 8.2E-07). Similar relationships were found between genetically driven histologic NAFLD with decreased BMI ( $\beta$  -0.0071; 95% CI -0.012 to -0.0023;  $p$  = 3.4E-03) but increased WHRadjBMI ( $\beta$  0.0072; 95% CI 0.0022–0.012;  $p$  = 4.5E-03). Taken together, our analyses suggested a consistent negative causal relationship between NAFLD and generalized obesity (proxied by BMI), but a positive association with central or visceral obesity (proxied by WHRadjBMI).

We next investigated the causal effect of NAFLD on blood lipid levels including HDL cholesterol, low-density lipoprotein (LDL) cholesterol, total cholesterol (TC), and triglycerides (TGs). Our analyses demonstrated a significant negative correlation between genetically elevated hepatic fat and TC levels ( $\beta$  -0.12 SD; 95% CI -0.17 to -0.074;  $p$  = 3.3E-07) as well as the LDL-C levels ( $\beta$  -0.098 SD; 95% CI -0.14 to -0.053;  $p$  = 2.3E-05). These negative relationships also exist for histologic NAFLD ( $\beta$  -0.019 SD; 95% CI -0.033 to -0.0054;  $p$  = 6.8E-03; and  $\beta$  -0.014 SD, 95% CI -0.026 to -0.0012;  $p$  = 3.1E-02 for TC and LDL-C, respectively). No significant causal relationship was found with other lipids (Table 1). Taken together, our analysis demonstrated a causal role of genetically driven NAFLD on central fat accumulation and reduced circulating cholesterol, but not generalized obesity.

### Sensitivity analysis using additional NAFLD genetic risk variants

It is known that the horizontal pleiotropic effect of the genetic instruments may invalidate the MR analysis. This risk can be reduced by using multiple genetic variants as instruments.<sup>49</sup> For this reason, we first performed a *post hoc* analysis by separately examining the causal role of *PNPLA3* and *TM6SF2/NCAN* polymorphisms separately, which generated similar results on most phenotypes (Table S4). Moreover, we tested if adding more NAFLD risk variants would change the results of the causal inference. As shown in Tables S7–8, the MR estimates obtained using all 5 GWAS-identified NAFLD risk variants (*PNPLA3* rs738409, *NCAN* rs2228603, *GCKR* rs780094, *PPP1R3B* rs4240624, and *LYPLAL1* rs12137855) were largely consistent with that obtained using *PNPLA3* and *TM6SF2/NCAN* alone. Similarly, we re-estimated the causal relationships by incorporating all 7 known NAFLD risk variants (the aforementioned 5 variants plus *MBOAT-TMC4* rs641738 and *HSD17B13* rs6834314) using the UKBB samples. The results were still consistent with the original estimates in terms of the causal association between NAFLD and T2D, insulin resistance, BMI and WHRadjBMI (Table S9). This result further confirmed that the causal relationship between NAFLD and T2D or obesity is highly likely a general mechanism rather than a biased association driven by a specific genetic variant.

### Reverse MR to test the causal effects of T2D, obesity, and their related traits on NAFLD

To understand the causal relationships among the 3 diseases, we implemented MR analyses to test the existence of reverse or bidirectional causal relationships between T2D or obesity and NAFLD. We used the data from our newly performed GWAS on NAFLD as an outcome, with the DIAGRAM and GIANT summary data for T2D and obesity as exposures, respectively. We found that genetic predictors of T2D exert positive effects on NAFLD (OR 1.1; 95% CI 1.0–1.2;  $p$  = 1.67E-03) without evidence of significant heterogeneity ( $P_{\text{MR-PRESSOGlobal}}$  = 0.31,  $P_{\text{modified Q}}$  = 0.33) after removing outlier variants identified by MR-PRESSO (Table 2). Initial MR estimates without removing outliers were shown in Table S5. Consistent with the previous MR estimate,<sup>14</sup> we found BMI causally increased the NAFLD risk (OR 2.3; 95% CI 2.0–2.7;  $p$  = 1.4E-25), but with remaining heterogeneity ( $P_{\text{MR-PRESSOGlobal}}$  <2.5E-03,  $P_{\text{modified Q}}$  = 3.9E-03) after removing outliers. WHRadjBMI significantly increased NAFLD risk (OR 1.5; 95% CI 1.3–1.8;  $p$  = 1.1E-06) without significant heterogeneity ( $P_{\text{MR-PRESSOGlobal}}$  = 0.46,  $P_{\text{modified Q}}$  = 0.45). The circulating TG level also causally increased the NAFLD risk (OR 1.6; 95% CI 1.3–1.9;  $p$  = 5.1E-07), with a mild remaining heterogeneity ( $P_{\text{MR-PRESSOGlobal}}$  = 7.0E-03,  $P_{\text{modified Q}}$  = 7.8E-03). In summary, T2D, increased BMI and central obesity, as well as increased circulating TGs, likely causally increase the risk of NAFLD.

### Transgenic mice study on the relationship between NAFLD and susceptibility to T2D and obesity

To further examine the causal effect of NAFLD on T2D and obesity, we set out to induce hepatosteatosis and NASH using transgenic animal models expressing human *PNPLA3* isoforms, and during which, to observe the development of T2D and obesity phenotypes. To do so, we constructed mice models transduced with a bacterial artificial chromosome containing the *PNPLA3*-148I isoform (TghPNPLA3-I148I) or that was engineered to the *PNPLA3*-148M (TghPNPLA3-I148M) isoform. The mice were then fed with a previously established HSD for 4 weeks to induce hepatosteatosis.<sup>31</sup> To examine the effect of more severe NAFLD and NASH phenotypes on T2D or obesity, we also fed mice with a “Western diet” (the AMLN diet) for 20 weeks, which has previously been shown to establish NASH.<sup>45–48</sup>

After 4 weeks of HSD diet, the TghPNPLA3-I148M mice developed severe hepatosteatosis compared to their TghPNPLA3-I148I littermates or non-transgenic controls, characterized by significantly increased lipid droplet formation in the liver (Fig. S2A) as well as hepatic TG accumulation (Fig. S2B). Meanwhile, compared to the TghPNPLA3-I148I controls, the TghPNPLA3-I148M mice also demonstrated a trend of increased circulating glucose, but the insulin level remained unchanged (Fig. S3A, B). After 4 weeks of HSD diet feeding, the TghPNPLA3-I148M mice demonstrated no significant change in total body weight (Fig. S3C), with a marginal trend to reduced circulating TC (Fig. S3D,  $p$  = 0.038) but not circulating TG levels (Fig. S3E), compared to their TghPNPLA3-I148I littermates.

To examine the effect of NASH progression on the susceptibility to T2D and obesity, we fed the mice with the NASH-inducing AMLN diet for 20 weeks. The TghPNPLA3-I148M mice developed significantly more severe NAFLD/NASH phenotypes than the TghPNPLA3-I148I littermates, as characterized by increased inflammation and fibrosis (Fig. S4–7), confirming that *PNPLA3* I148M strongly predisposes to NAFLD and NASH. H&E



staining results indicated that all 3 groups had developed hepatosteatosis after 20 weeks of the AMLN diet (Fig. S7).

We then evaluated the effect of PNPLA3-I148M on glucose homeostasis over a 20-week follow-up in the cohort fed with the AMLN diet. As shown in Fig. 2A, we observed a significant genotype-time interaction on the fasting glucose level (2-way repeated measure ANOVA,  $p < 0.0001$ ), suggesting that the effect of PNPLA3-I148M on glucose levels depended on disease progression. At week 16 and 18, the TghPNPLA3-I148M mice displayed significantly higher fasting glucose levels than their TghPNPLA3-I148I littermates ( $p = 0.0048$  and  $0.0082$ , respectively). There is also a significant interaction between genotype and time on fasting insulin levels between the TghPNPLA3-I148I and TghPNPLA3-I148M groups ( $p = 0.0009$ ). However, there is no significant difference between the TghPNPLA3-I148M and non-transgenic wild-type mice. Beginning at week 12, the insulin levels between the latter 2 groups remain unchanged (Fig. 2B). Results of the glucose tolerance test (GTT) showed that TghPNPLA3-I148M mice experienced a reduced clearance of blood glucose compared to the TghPNPLA3-I148I controls ( $p = 0.012$ ) (Fig. 2C). However, we did not observe a significant genotypic difference in response to insulin challenge in the insulin tolerance test (ITT) (Fig. 2D).

The body weight change of the mice on the AMLN diet over time was shown in Fig. 2E. The TghPNPLA3-I148M mice were significantly lighter than the TghPNPLA3-I148I controls beginning at week 15 (all  $p < 0.05$ ). MRI examination at week 20 showed that less total fat was accumulated in the TghPNPLA3-I148M mice than the TghPNPLA3-I148I controls ( $p = 0.012$ ), while the lean mass of non-fat tissues was not significantly different (Fig. 2F). Further investigation on the composition of the isolated fat showed that there was a significantly more epididymal white adipose tissue (eWAT) accumulation relative to the total peripheral adipose tissue in the TghPNPLA3-I148M mice than their TghPNPLA3-I148I littermates or non-transgenic controls ( $p = 0.034$  and  $0.0015$ , respectively) (Fig. 2G). Examining the plasma lipid profile showed a significant decrease in TC levels beginning at week 16 in TghPNPLA3-I148M mice compared to the TghPNPLA3-I148I controls (Fig. 2H). No significant difference in circulating TG levels between the 3 groups were observed (Fig. 2I). The representative image of the mice after 20 weeks of AMLN diet feeding was shown in Fig. 2J.

#### Assessment of insulin and glucagon signals and inflammatory status of the mouse pancreas

The increased glucose level, reduced glucose clearance and the lower level of insulin in the TghPNPLA3-I148M mice compared to the TghPNPLA3-I148I controls suggested a potentially lower pancreatic secretion of insulin in the TghPNPLA3-I148M mice. To verify this, we stained the insulin and glucagon signals in the pancreas tissue of all 3 groups of mice. Immunofluorescence assays revealed significantly less insulin but higher glucagon staining in the pancreas of TghPNPLA3-I148M mice than in the TghPNPLA3-I148I mice ( $p = 0.0149$  and  $p = 0.0197$ , respectively) (Fig. 3A).

In order to further understand the underlying reason for imbalanced insulin and glucagon signals in the islets, we hypothesized that the central organ fat accumulation promoted by PNPLA3-I148M may increase chronic inflammation in the pancreas. To test this hypothesis, we stained the murine macrophage marker F4/80 using immunofluorescence in the

pancreas. Indeed, the analysis revealed that the F4/80<sup>+</sup> staining signals were significantly more abundant in the pancreas of the TghPNPLA3-I148M mice than the TghPNPLA3-I148I littermates ( $p = 0.0111$ ) (Fig. 3B), though no significant distribution of the F4/80<sup>+</sup> signals within or around the islets were observed (data not shown). Taken together, these data indicated that increased chronic pancreatic inflammation may lead to decreased insulin but increased glucagon secretion in the TghPNPLA3-I148M mice compared to the TghPNPLA3-I148I controls.

#### Akt signaling in mouse liver and muscle tissues

In order to further investigate the insulin signaling in these 3 groups mice, hepatic and muscle Akt phosphorylation levels were examined using western blotting. The results showed that phosphorylation of Akt (pSer473) signal in TghPNPLA3-I148M group was marginally increased in the liver ( $p = 0.0079$ ) but not in the muscle tissues compared to their TghPNPLA3-I148I littermates (Fig. 3C), suggesting that TghPNPLA3-I148M mice were not more likely to develop tissue insulin resistance on the AMLN diet.

#### Transcriptional changes of the thermogenesis and cholesterol metabolism pathways in adipose and liver tissues, respectively

We further set out to understand the potential mechanism underlying the reduced body weight but increased central fat accumulation in the TghPNPLA3-I148M mice. Previous studies have demonstrated that thermogenesis is a physiological defense against obesity that limits weight gain in response to metabolic stress.<sup>50,51</sup> We thus measured and compared the expression level of key thermogenic pathway genes in the intrascapular brown adipose tissue (iBAT), eWAT and subcutaneous white adipose tissue (scWAT) of the 3 groups mice. The results showed that there was significantly increased expression of thermogenic marker genes in iBAT (*Ucp-1* and *Nrf1*) and scWAT (*Ucp-1*, *Nrf1* and *cox8b*) ( $p < 0.05$  for all tests) but not in eWAT of the TghPNPLA3-I148M mice compared to their TghPNPLA3-I148I littermates (Fig. 3D). This result suggested that the body weight loss in TghPNPLA3-I148M mice may be attributed to, at least in part, the activation of thermogenesis in both iBAT and scWAT.

To further understand the mechanism underlying the lower circulating TC in the TghPNPLA3-I148M mice, we measured the expression of genes involved in hepatic cell transporting (*Ldlr*, *Myliip*), cholesterol biosynthesis (*Sqle*, *Lss*, *Fdft1*, *Hmgcs1*, *Soat2*, *Dhcr7*, *Scd5*, *Nsdh1*, *Hsd17b7*, and *Cyp51*) and cholesterol secretion (*Tm7sf2*, *Abcg1*, *Abca1* and *Apob*). We found that while there is no significant change in the expression of genes involved in cholesterol transporting and secretion, the expression of multiple genes involved in cholesterol biosynthesis were significantly downregulated in the TghPNPLA3-I148M mice compared to the wild-type groups ( $p < 0.05$  for all tests) (Fig. 3E).

#### Discussion

This is the first large-scale study to simultaneously delineate the causal inter-relationship between NAFLD, T2D, and obesity using a 2-sample and bidirectional MR analysis. The findings were also experimentally validated using an established genetic murine model of NAFLD, which largely corroborated the causal relationship between NAFLD and the susceptibility to T2D and obesity observed in humans. Overall, we found that genetically driven NAFLD is a causal risk factor for T2D which has a unique



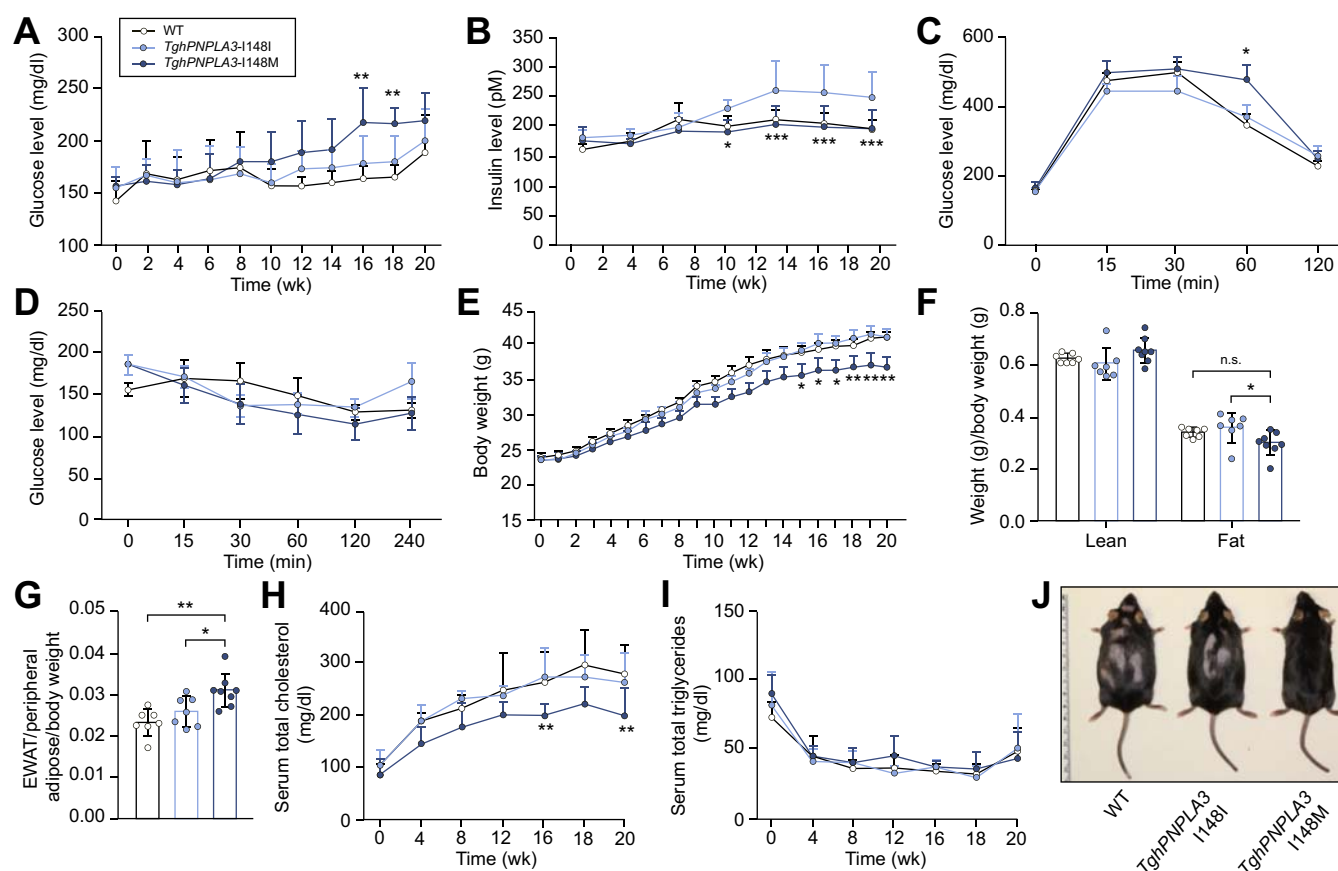


**Fig. 2. Phenotypic changes of the mice fed with an AMLN diet.** (A) Change in glucose levels over time of TghPNPLA3-I148I, TghPNPLA3-I148M, and non-transgenic wide type mice fed with an AMLN diet for 20 weeks. Error bar represents SD. The significance level of the comparison between TghPNPLA3-I148I and TghPNPLA3-I148M was indicated as follows: \*\* $p < 0.01$ , ANOVA with Tukey's multiple comparison test; (B) Change in insulin levels for 20 weeks. Error bar represents SD. The significance level of the comparison between TghPNPLA3-I148I and TghPNPLA3-I148M was indicated as follows: \* $p < 0.05$ , \*\*\* $p < 0.001$ , ANOVA with Tukey's multiple comparison test; (C) GTT, Error bar represents SD. The significance level of the comparison between TghPNPLA3-I148I and TghPNPLA3-I148M was indicated as follows: \* $p < 0.05$ , ANOVA with Tukey's multiple comparison test; and (D) ITT were performed at the 16th week of high-fat complex carbohydrate diet feeding. Error bar represents SD, ANOVA with Tukey's multiple comparison test, all  $p > 0.05$ ; (E) Change in body weight of TghPNPLA3-I148I, TghPNPLA3-I148M, and non-transgenic wide type mice fed with the AMLN diet for 20 weeks. Error bar represents SD. The significance level of the comparison between TghPNPLA3-I148I and TghPNPLA3-I148M was indicated as follows: \* $p < 0.05$ , \*\* $p < 0.01$ , ANOVA with Tukey's multiple comparison test; (F) Body composition analysis by MRI. Fat tissue weight and non-fat lean mass were normalized by the body weight. Error bar represents SD. The significance level was indicated as follows: \* $p < 0.05$ , ns: not significant, ANOVA with Tukey's multiple comparison test; (G) EWAT accumulation at the 20th week of AMLN diet feeding. EWAT accumulation was calculated as weight of EWAT normalized by the total peripheral adipose tissue weight and then further normalized by the body weight. Error bar represents SD. The significance level was indicated as follows: \* $p < 0.05$ , \*\* $p < 0.01$ , ANOVA with Tukey's multiple comparison test; (H) Change in serum TC levels over 20 weeks. Error bar represents SD. The significance level of the comparison between TghPNPLA3-I148I and TghPNPLA3-I148M was indicated as follows: \*\* $p < 0.01$ , ANOVA with Tukey's multiple comparison test; (I) Change in serum total triglycerides levels over 20 weeks. Error bar represents SD. ANOVA with Tukey's multiple comparison test, all  $p > 0.05$ ; (J) The representative image of TghPNPLA3-I148I, TghPNPLA3-I148M, and non-transgenic wide type mouse after 20 weeks of AMLN diet feeding. Sample size: TghPNPLA3-I148I ( $n = 7$ ), TghPNPLA3-I148M ( $n = 8$ ), and non-transgenic wide type ( $n = 7$ ). AMLN, high-fat, high-fructose and high-cholesterol; EWAT, epididymal white adipose tissue; GTT, glucose tolerance test; ITT, insulin tolerance test. (This figure appears in color on the web.)

phenotype characterized by normal insulin sensitivity but reduced insulin secretion (a late-onset type I-like diabetic phenotype). The genetically driven NAFLD also protects against overall or generalized obesity (indexed by BMI), but increases the risk of central obesity. Genetically driven T2D and central or generalized obesity all causally increase the risk of NAFLD. Our study suggests that genetically driven NAFLD is likely a "lipodystrophic NAFLD" phenotype characterized by reduced peripheral but increased central fat accumulation, with a normal or low circulating lipid profile. This phenotype may be distinct from the NAFLD that is metabolically driven by T2D, obesity and/or increased TG, thus a "metabolic NAFLD" subphenotype. Our findings hence reveal new insights into how nature and nurture

underpin these 3 diseases, providing strong evidence for disease subphenotyping.

NAFLD and NASH have long been regarded as the central manifestations of T2D and obesity. Due to the lack of data on the natural history of NAFLD/NASH in humans, the causal relationship between NAFLD and T2D or obesity has remained largely unclear. Addressing this issue is of critical importance for patient stratification, clinical management, drug discovery and development. For the first time, our study dissected the 3 diseases into important subtypes. First, we observed that genetically driven NAFLD is a causal risk factor for T2D. Our study confirmed the findings of a previous small-scale MR analysis,<sup>12</sup> and is in line with the results of numerous observational studies, including a

recent meta-analysis of 19 observational studies with 296,439 individuals which indicated that patients with NAFLD had a 2-fold higher risk of developing T2D than those without NAFLD.<sup>3</sup> Interestingly, while a strong causal effect between NAFLD and T2D was observed, there was no significant causal relationship between genetic NAFLD and insulin resistance. This observation in human data was confirmed in the animal study: there is no genotypic difference in the glucose level in response to insulin as demonstrated in the ITT assay (Fig. 2D). Also, no evidence of tissue insulin resistance was observed. While in humans there is no strong causal association between PNPLA3-148M and other glycemic traits, the PNPLA3-148M mice demonstrated hyperglycemia and prolonged glucose clearance in the GTT assay. Why is there such a dissociation between T2D and insulin resistance, and why are there discrepancies between humans and mice? There are a few possibilities: First, the glucose disturbance associated with PNPLA3-driven NAFLD may be an atypical T2D phenotype, thus a disease subtype. Indeed, in our animal study, we found that the circulatory insulin level showed a significant decrease in the 148M mice compared to the 148I mice after 12 weeks (Fig. 2B). We found that the stained insulin signal in the pancreas was significantly lower in the 148M than the 148I mice, while the glucagon signal was higher in the 148M mice than the 148I mice (Fig. 3A), suggesting an imbalanced pancreatic production of insulin and glucagon in the 148M mice. We further hypothesize that this may be due to chronic pancreatic inflammation given the increased central organ fat accumulation associated with this model. By staining for F4/80, a murine macrophage marker in the pancreas, we found that the pancreatic inflammation level of the 148M mice was indeed significantly higher than that of the 148I mice (Fig. 3B). Therefore, it seems that PNPLA3-148M may lead to increased chronic pancreatic inflammation, which further alters the balance of insulin/glucagon secretion. This resembles a type I-like diabetes phenotype. This finding is consistent with the normal insulin sensitivity of the PNPLA3-148M mice compared to their wild-type littermates in the ITT assay (Fig. 2D). In fact, the dissociation between the PNPLA3-148M-driven hepatic steatosis and insulin resistance has been consistently observed among human populations but lacks a clear mechanism.<sup>26,52–54</sup> Our animal study provides new evidence to this question.

Second, in contrast to a well-controlled animal study, in human populations metabolic markers *e.g.* glucose, insulin, or HbA1c are more likely modified by other factors, *e.g.* medications, comorbidities or other disease conditions. Medication intake may normalize these markers and thus weaken the genetic association. Meanwhile, insulin levels and insulin resistance status could be further modified by other disease conditions, *e.g.* systemic obesity. Co-existence of various risk factors in PNPLA3-148M individuals may also increase susceptibility to obesity, which may further lead to elevated insulin resistance, thus compromising the normal insulin sensitivity conferred by PNPLA3-148M. This may explain the mixed results obtained to date, regarding the association between PNPLA3-148M and insulin resistance. If this is true, then individuals carrying 148M without obesity or metabolic stresses would maintain a normal response to insulin. Indeed, in a large-scale study by Palmer *et al.*,<sup>55</sup> the association between the 148M allele and insulin resistance disappeared among individuals after bariatric surgery, and no association was observed among obese individuals with BMI <35. Taken together, these data suggest that

the PNPLA3-driven NAFLD may lead to a late-onset type I-like diabetes that is distinct from typical T2D. Increasing evidence has demonstrated that type 1 diabetes (T1D) may commonly (40–50% of all T1D) occur in adulthood, and these patients are often misdiagnosed and treated as T2D, which can lead to serious clinical consequences.<sup>56,57</sup> Interestingly, in humans, late-onset T1D is significantly associated with low BMI,<sup>56</sup> mirroring the observations in our study. However, whether the phenotypes we have observed in our study match the typical late-onset T1D defined in humans requires further confirmation. Confirmation would help stratify patients with T2D who require different clinical management. Our data again highlight the importance of disease subphenotyping.

Our study also revealed an interesting relationship between NAFLD and obesity. Although obesity is highly correlated with NAFLD epidemiologically, genetically driven NAFLD is not a causal risk factor for overall obesity. Rather, it protects against overall BMI elevation. However, genetically driven NAFLD causally increases the risk of central obesity, characterized as an increased WHR in humans. Our analysis suggests that genetically driven NAFLD may promote the remodeling of fat distribution in the whole body. This finding is consistent with numerous observational studies on the associations between NAFLD, visceral fat or WHR and BMI,<sup>58,59</sup> and corroborates the widely discussed hypothesis about “lean NAFLD” and “obese NAFLD”.<sup>60,61</sup> Our study echoes this observation and indicates that genetically driven NAFLD may be more likely to progress to “lean” (given the low BMI) NAFLD, which does not promote the development of overall obesity, and can therefore be considered “lipodystrophic NAFLD”. This is also consistent with the observation that lean NAFLD is associated with adipose tissue dysfunction, impaired glucose tolerance, and the PNPLA3 I148M allele.<sup>60,61</sup> Our mouse study accurately recapitulated these relationships. Further mechanistic analyses revealed that thermogenic pathway gene expression was significantly upregulated in subcutaneous white adipose tissue and brown adipose tissue but not in epididymal fat, suggesting that the TgHPNPLA3-I148M mice may exhibit increased thermogenesis by turning subcutaneous fat into heat. This is the first report of the effect of PNPLA3-148M on adipose tissue browning or thermogenesis. We postulate that this increased visceral fat accumulation and activated thermogenesis in the subcutaneous fat may reflect a genetic adaption to cold stress during human evolution and migration, given the dramatically increased PNPLA3-148M allele frequency from Africans (<10%) to Eurasians (20–40%) and Native Americans (70–80%).<sup>62</sup> A schematic representation of this mechanism is shown in Fig. 4. The underlying mediator for this genotype-specific activation of thermogenesis remains unclear.

Another interesting observation in our study is that both the MR and animal data indicated that genetic NAFLD causally decreases circulating cholesterol (TC and LDL-C). This phenotype was similar in mice fed with either HSD or the AMLN diet, suggesting a diet-independent mechanism. Mechanistically, this may be related to the hepatic very low-density lipoprotein retention associated with PNPLA3-148M, as previously observed.<sup>63</sup> After profiling the key genes involved in cholesterol metabolism in the liver, we found that the cholesterol biosynthesis pathway genes were particularly downregulated. Therefore, central obesity, at least in part, may possess a subtype attributed to genetically driven NAFLD. This is particularly significant, as both TC and TG are generally correlated with visceral

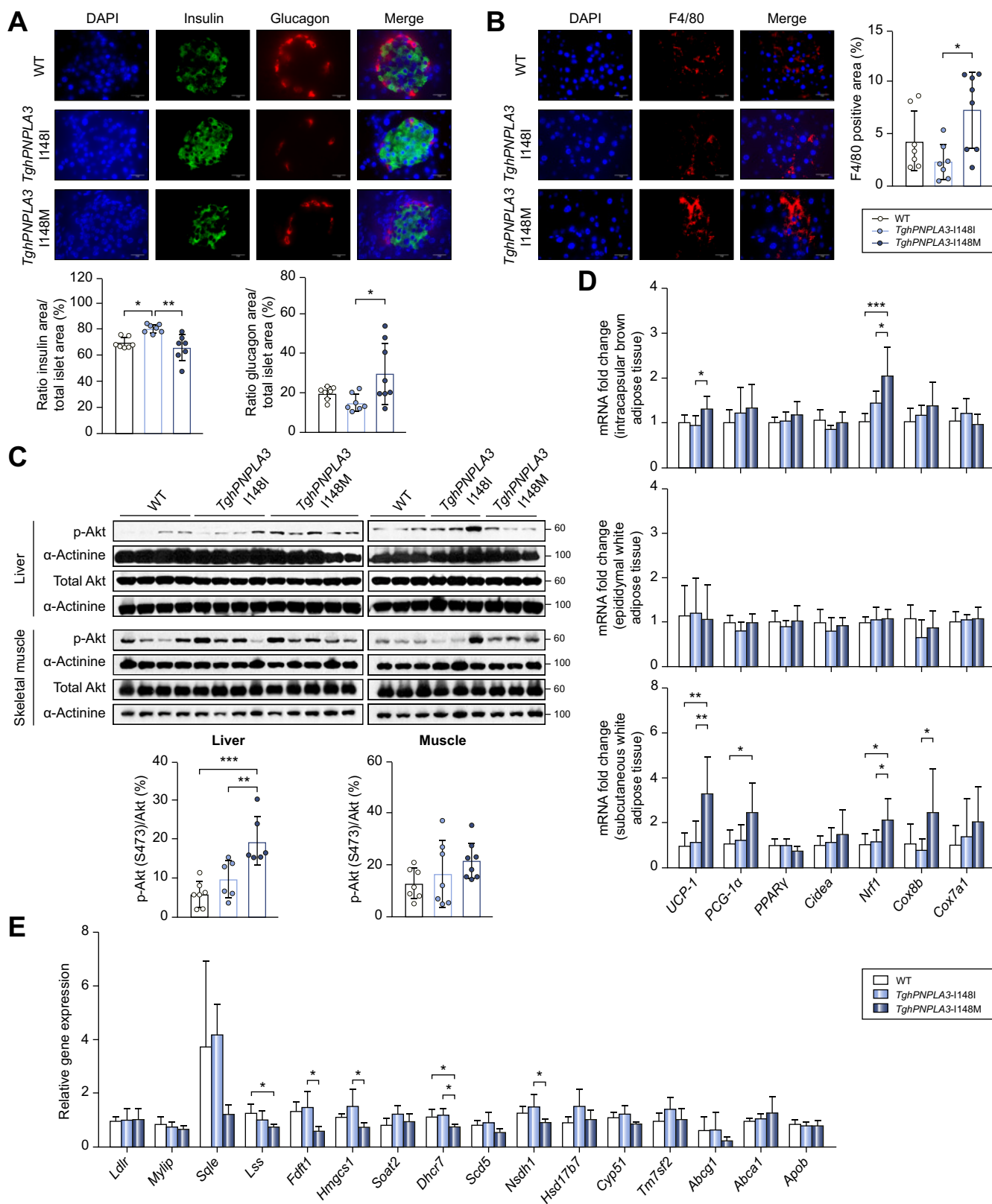


**Fig. 3. Underlying mechanism of PNPLA3 I148M in regulating pancreas function and inflammation, as well as adipose thermogenic and hepatic cholesterol metabolism pathways.** (A) Immunofluorescence double staining to identify insulin and glucagon secretion with antibodies against insulin (green) and glucagon (red) in non-transgenic wild-type, TghPNPLA3-I148I or TghPNPLA3-I148M mouse pancreas. Nuclei were labeled with DAPI (blue). Scale bars: 20  $\mu$ m, 630x magnification. The quantifications of area of stained insulin and glucagon signals were shown below. Error bar represents SD. The significance level was indicated as follows: \* $p$  < 0.05, \*\* $p$  < 0.01, ANOVA with Tukey's multiple comparison test; (B) Immunofluorescence staining for macrophage marker F4/80 (red) in

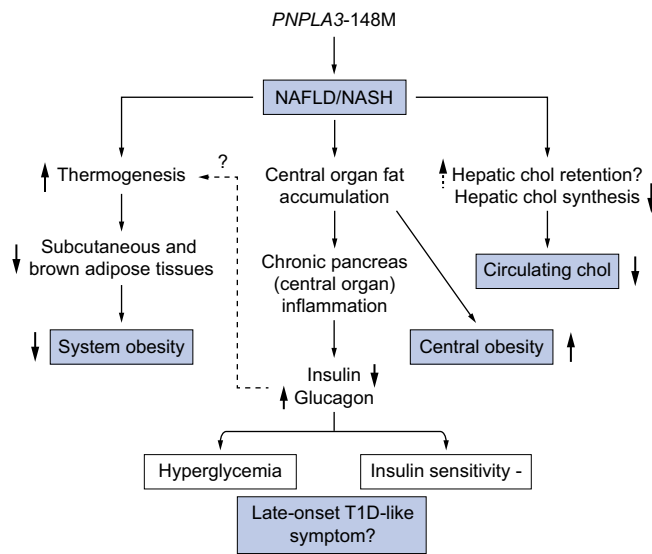


**Fig. 4. Schematic summary of the causal relationship between *PNPLA3*-148M driven NAFLD and obesity, diabetes and cholesterol metabolism.** NAFLD, non-alcoholic fatty liver disease; NASH, non-alcoholic steatohepatitis.

fat accumulation.<sup>64,65</sup> The dissociation observed in our study suggests that the NAFLD-driven central obesity is likely a unique subphenotype as well.

Our findings also demonstrated that T2D, obesity (both generalized and central) and increased TG are likely causal risk factors for NAFLD, though certain pleiotropic effects may remain. This is not surprising. First, hyperglycemia and adiposity could amplify or modify the effect of genetic risk factors to promote the development of NAFLD. High glucose levels can increase the expression of *PNPLA3* by regulating carbohydrate-response element-binding protein (ChREBP),<sup>66</sup> which is a necessary step for the accumulation of *PNPLA3*-148M protein on the surface of lipid droplets in hepatocytes.<sup>30,31,67</sup> This accumulation further alters the dynamics of triglyceride hydrolysis and leads to hepatic steatosis.<sup>68</sup> Similarly, adiposity has also been demonstrated to synergize the effects of genetic risk factors on the development of NASH or more severe liver injuries.<sup>14</sup> Second, impaired glucose perturbation and adiposity can also increase the risk of NAFLD independently of genetic risk factors. Numerous studies in humans have shown that NAFLD and NASH can be developed among T2D or obese individuals carrying wild-type genotypes of *PNPLA3* or other genetic variants.<sup>69</sup> Many diet-induced animal models without genetic modification also develop NAFLD/NASH.<sup>45–48</sup> In this case, NAFLD/NASH should be a comorbidity of

T2D or obesity. This highlights the impact of “nurture” on the development of NAFLD.

Taken together, our study suggests that NAFLD should be re-classified into at least 2 subtypes: i) “genetic NAFLD” (nature) which is characterized by central fat deposition (lipodystrophy), type 1-like diabetic symptom without insulin resistance as well as normal or low lipid profile; and ii) “metabolic NAFLD” (nurture) which is a comorbidity of diabetes mellitus and/or obesity. Distinguishing these 2 subtypes may have important clinical implications. First, as the genetically driven NAFLD generally has a low or normal BMI (thus generally “lean”) and lipid profile, Individuals with this subtype may seem to be “healthier” than the “metabolic NAFLD”. For this reason, they may be under diagnosed for their liver injuries. This is a particular issue, as patients with “lean” NAFLD can present with a more advanced liver histology than their obese counterparts.<sup>70</sup> Second, distinguishing the 2 subtypes would be critical for precision treatment of NAFLD/NASH given the currently limited therapeutic strategy. Given the different causes for the 2 subtypes, designing treatments for genetic NAFLD should be focused on the causal genes and underlying pathways. To this end, genotype-based targeted therapies would be an intriguing direction of research.<sup>71</sup> Indeed, recent *PNPLA3*-targeting strategies have demonstrated promising results in ameliorating NASH in mice.<sup>72</sup> Similar investigations are currently ongoing in our group as well. Meanwhile, metabolic NAFLD should be managed by focusing on the metabolic disease, e.g. to reduce the body weight. These new hypotheses should be examined in future studies.

It is worth noting that our MR analyses, using various combinations of multiple genetic variants as instruments, generated similar results regarding the causal relationships between NAFLD, T2D, obesity as well as insulin resistance. This strongly suggests that these causal relationships are general to all genetically driven NAFLD rather than a biased association caused by a specific gene (e.g. due to horizontal pleiotropy). Of course, it is still possible that the mechanisms underlying these relationships observed in our animal study is specific to *PNPLA3*. Notably, our collaborator's (co-author Y.E.C) unpublished work on a mouse model expressing the *TM6SF2* variant also demonstrated a similar phenotype. In addition, although we used the largest-to-date dataset for our analysis, we only focused on using hepatic steatosis or binary histologic NAFLD as exposures. Previous studies demonstrated that severity of liver damage may lead to different causal impact on other metabolic diseases. Therefore, it would be important to dissect the severity of NAFLD to further delineate the potential causal impact on other perturbations. Unfortunately, there is a lack of sufficient high quality GWAS data on well-characterized NAFLD/NASH especially in large cohorts. Future studies should further explore this question.

non-transgenic wild-type, Tgh*PNPLA3*-I148I and Tgh*PNPLA3*-I148M mouse pancreas. Nuclei were labeled with DAPI (blue). Scale bars: 20  $\mu$ m, 630x magnification. The quantification of F4/80-positive area was shown in the right. The positive area was measured in randomly selected fields (3 fields per section). Error bar represents SD. The significance level was indicated as follows: \* $p$  < 0.05, ANOVA with Tukey's multiple comparison test; (C) Western blot analysis of the level of total and phospho-Akt (Ser473) proteins in liver and skeletal muscle tissue.  $\alpha$ -Actinin was used as the loading control. The densitometry ratio of the expression of p-Akt and total Akt was demonstrated below. Error bar represents SD. The significance level was indicated as follows: \*\* $p$  < 0.01, \*\*\* $p$  < 0.001, ANOVA with Tukey's multiple comparison test; (D) Fold change in expression of thermogenic genes in interscapular brown adipose tissue, epididymal white adipose tissue and subcutaneous white adipose tissue. Error bar represents SD. The significance level was indicated as follows: \* $p$  < 0.05, \*\* $p$  < 0.01, \*\*\* $p$  < 0.001, ANOVA with Tukey's multiple comparison test; (E) Fold change in the cholesterol metabolism-related gene expression in liver. Error bar represents SD. The significance level was indicated as follows: \* $p$  < 0.05, ANOVA with Tukey's multiple comparison test. Sample size: Tgh*PNPLA3*-I148I ( $n$  = 7), Tgh*PNPLA3*-I148M ( $n$  = 8), and non-transgenic wild-type ( $n$  = 7).



In summary, our study combined both a large-scale bidirectional MR analysis and animal models to delineate the causal relationships between NAFLD, T2D, and obesity. Our findings provide strong evidence for disease subphenotyping and foster new hypotheses for the development of precision diagnostic, preventive and therapeutic strategies for the 3 diseases. The *PNPLA3*-specific study demonstrated that the 148M variant leads to NAFLD and central organ fat accumulation, which may result in chronic tissue inflammation, altering insulin/glucagon signaling and further reducing glucose tolerance. Meanwhile, genetic NAFLD may also promote browning and thermogenesis of peripheral adipose tissue, while maintaining a normal circulating lipid profile. Together with central fat deposition, this pattern may reflect a general defensive mechanism against cold stress during human evolution and migration.

### Abbreviations

ALT, alanine aminotransferase; AST, aspartate aminotransferase; AUCins, AUC of insulin levels during oral glucose tolerance test; AUCins/AUCgluc, ratio of AUC insulin and AUC glucose; BMI, body mass index; CIRadjBMI, corrected insulin response adjusted for ISI; DI, disposition index; GWAS, genome-wide association study; HDL-c, high-density lipoprotein cholesterol; HOMA-B, homeostatic model assessment of beta cell function; HOMA-IR, homeostatic model assessment of insulin resistance; Ins30adjBMI, insulin response to glucose during the first 30 min adjusted for BMI; Incre30, incremental insulin at 30 min; ISI, insulin sensitivity index; ITT, insulin tolerance test; IVW, inverse variance weighted; LDL-c, low-density lipoprotein cholesterol; MR, Mendelian randomization; OGTT, oral glucose tolerance test; OR, odds ratio; SNPs, single nucleotide polymorphisms; T1D, type 1 diabetes; T2D, type 2 diabetes; TC, total cholesterol; TGs, triglycerides; UKBB, UK Biobank; WHR, waist-hip ratio; WHRadjBMI, WHR adjusted for BMI.

### Financial support

This study is supported in part by the NIH/NIDDK grant (R01DK106540) (W.L.), and the start-up fund of the Office of Vice President for Research of Wayne State University (W.L.), NIH R21AA024550 (X.C.D.), R01DK091592 (X.C.D.), R56DK091592 (X.C.D.), Indiana Diabetes Research Center grant NIH P30DK097512, and the Indiana Clinical and Translational Sciences Institute funded from the NIH NCATS CTSA UL1TR002529. D.C. is a visiting scholar supported by the Shenzhen Children's Hospital, Shenzhen, China.

### Conflict of interest

All authors have reviewed the manuscript. C.W.'s spouse works at Regeneron Pharmaceuticals, and all other co-authors declared no conflict of interest. The sponsor of the study has no role in the study design, collection, analysis, and interpretation of data.

Please refer to the accompanying [ICMJE disclosure](#) forms for further details.

### Authors' contributions

Conceptualization: W.L.; Methodology: Z.L., Y.Z., and S.G.; Formal Analysis: Z.L.; Investigation: Z.L., Y.Z., S.G., X.W., D.C., and M.H.; Writing—Original Draft: Z.L., Y.Z. and W.L.; Writing—Review & Editing: Z.L., Y.Z., S.G., R.P., X.C.D., Y.E.C., C.W., and W.L.; Funding Acquisition: X.C.D. and W.L.; Supervision: W.L.

### Acknowledgements

We thank all the genetics consortiums for making the GWAS summary data publicly available. We would also like to thank Drs. Anjaneyulu Kowluru and James Granneman, as well as Jean-Christophe Rochet and his group for their insightful discussion and comments on this study.

### Supplementary data

Supplementary data to this article can be found online at <https://doi.org/10.1016/j.jhep.2020.03.006>.

### References

*Author names in bold designate shared co-first authorship*

- [1] Chalasani N, Younossi Z, Lavine JE, Charlton M, Cusi K, Rinella M, et al. The diagnosis and management of nonalcoholic fatty liver disease: Practice guidance from the American Association for the Study of Liver Diseases. *Hepatology* 2018;67:328–357.
- [2] Hardy T, Oakley F, Anstee QM, Day CP. Nonalcoholic fatty liver disease: pathogenesis and disease spectrum. *Annu Rev Pathol* 2016;11:451–496.
- [3] Mantovani A, Byrne CD, Bonora E, Targher G. Nonalcoholic fatty liver disease and risk of Incident type 2 diabetes: a meta-analysis. *Diabetes Care* 2018;41:372–382.
- [4] **Hu M, Phan F**, Bourron O, Ferre P, Foulle F. Steatosis and NASH in type 2 diabetes. *Biochimie* 2017;143:37–41.
- [5] **Lonardo A, Lugari S, Ballestri S, Nascimbeni F, Baldelli E, Maurantonio M**. A round trip from nonalcoholic fatty liver disease to diabetes: molecular targets to the rescue? *Acta Diabetol* 2019;56:385–396.
- [6] Loomis AK, Kabadi S, Preiss D, Hyde C, Bonato V, St Louis M, et al. Body mass index and risk of nonalcoholic fatty liver disease: two electronic health record prospective studies. *J Clin Endocrinol Metab* 2016;101:945–952.
- [7] Fabbri E, Sullivan S, Klein S. Obesity and nonalcoholic fatty liver disease: biochemical, metabolic, and clinical implications. *Hepatology* 2010;51:679–689.
- [8] Lawlor DA, Harbord RM, Sterne JAC, Timpson N, Smith GD. Mendelian randomization: using genes as instruments for making causal inferences in epidemiology. *Stat Med* 2008;27:1133–1163.
- [9] **Voight BF, Peloso GM**, Orho-Melander M, Frikke-Schmidt R, Barbalic M, Jensen MK, et al. Plasma HDL cholesterol and risk of myocardial infarction: a mendelian randomisation study. *Lancet* 2012;380:572–580.
- [10] Paternoster L, Tilling K, Smith GD. Genetic epidemiology and Mendelian randomization for informing disease therapeutics: conceptual and methodological challenges. *PLoS Genet* 2017;13:e1006944.
- [11] Welsh P, Polisecki E, Robertson M, Jahn S, Buckley BM, de Craen AJM, et al. Unraveling the directional link between adiposity and inflammation: a bidirectional mendelian randomization approach. *J Clin Endocrinol Metab* 2010;95:93–99.
- [12] **Dongiovanni P, Stender S, Pietrelli A, Mancina RM**, Cespiati A, Petta S, et al. Causal relationship of hepatic fat with liver damage and insulin resistance in nonalcoholic fatty liver. *J Intern Med* 2018;283:356–370.
- [13] **De Silva NMG, Borges MC**, Hingorani A, Engmann J, Shah T, Zhang X, et al. Liver function and risk of type 2 diabetes: bidirectional Mendelian randomization study. *Diabetes* 2019;68:1681–1691.
- [14] Stender S, Kozlitina J, Nordestgaard BG, Tybjaerg-Hansen A, Hobbs HH, Cohen JC. Adiposity amplifies the genetic risk of fatty liver disease conferred by multiple loci. *Nat Genet* 2017;49:842–847.
- [15] **Speliotes EK, Yerges-Armstrong LM, Wu J, Hernaez R, Kim LJ**, Palmer CD, et al. Genome-wide association analysis identifies variants associated with nonalcoholic fatty liver disease that have distinct effects on metabolic traits. *PLoS Genet* 2011;7:e1001324.
- [16] Mahajan A, Taliun D, Thurner M, Robertson NR, Torres JM, Rayner NW, et al. Fine-mapping type 2 diabetes loci to single-variant resolution using high-density imputation and islet-specific epigenome maps. *Nat Genet* 2018;50:1505–1513.
- [17] **Wheeler E, Leong A**, Liu CT, Hivert MF, Strawbridge RJ, Podmore C, et al. Impact of common genetic determinants of hemoglobin A1c on type 2 diabetes risk and diagnosis in ancestrally diverse populations: a trans-ethnic genome-wide meta-analysis. *PLoS Med* 2017;14:e1002383.
- [18] **Manning AK, Hivert MF, Scott RA**, Grimsby JL, Bouatia-Naji N, Chen H, et al. A genome-wide approach accounting for body mass index identifies

- genetic variants influencing fasting glycemic traits and insulin resistance. *Nat Genet* 2012;44:659–669.
- [19] **Strawbridge RJ, Dupuis J, Prokopenko I, Barker A, Ahlqvist E, Rybin D, et al.** Genome-wide association identifies nine common variants associated with fasting proinsulin levels and provides new insights into the pathophysiology of type 2 diabetes. *Diabetes* 2011;60:2624–2634.
  - [20] **Saxena R, Hivert MF, Langenberg C, Tanaka T, Pankow JS, Vollenweider P, et al.** Genetic variation in GIPR influences the glucose and insulin responses to an oral glucose challenge. *Nat Genet* 2010;42:142–148.
  - [21] **Dupuis J, Langenberg C, Prokopenko I, Saxena R, Soranzo N, Jackson AU, et al.** New genetic loci implicated in fasting glucose homeostasis and their impact on type 2 diabetes risk. *Nat Genet* 2010;42:105–116.
  - [22] **Prokopenko I, Poon W, Magi R, Prasad BR, Salehi SA, Almgren P, et al.** A central role for GRB10 in regulation of islet function in man. *PLoS Genet* 2014;10:e1004235.
  - [23] **Pulit SL, Stoneman C, Morris AP, Wood AR, Glastonbury CA, Tyrrell J, et al.** Meta-analysis of genome-wide association studies for body fat distribution in 694 649 individuals of European ancestry. *Hum Mol Genet* 2019;28:166–174.
  - [24] **Willer CJ, Schmidt EM, Sengupta S, Peloso GM, Gustafsson S, Kanoni S, et al.** Discovery and refinement of loci associated with lipid levels. *Nat Genet* 2013;45:1274–1283.
  - [25] **Zhou W, Nielsen JB, Fritsche LG, Dey R, Gabrielsen ME, Wolford BN, et al.** Efficiently controlling for case-control imbalance and sample relatedness in large-scale genetic association studies. *Nat Genet* 2018;50:1335–1341.
  - [26] **Romeo S, Kozlitina J, Xing C, Pertsemlidis A, Cox D, Pennacchio LA, et al.** Genetic variation in *PNPLA3* confers susceptibility to nonalcoholic fatty liver disease. *Nat Genet* 2008;40:1461–1465.
  - [27] **Kozlitina J, Smagris E, Stender S, Nordestgaard BG, Zhou HH, Tybjaerg-Hansen A, et al.** Exome-wide association study identifies a *TM6SF2* variant that confers susceptibility to nonalcoholic fatty liver disease. *Nat Genet* 2014;46:352–356.
  - [28] **Liu YL, Reeves HL, Burt AD, Tiniakos D, McPherson S, Leathart JB, et al.** *TM6SF2* rs58542926 influences hepatic fibrosis progression in patients with non-alcoholic fatty liver disease. *Nat Commun* 2014;5:4309.
  - [29] **Wang X, Liu Z, Wang K, Wang Z, Sun X, Zhong L, et al.** Additive effects of the risk alleles of *PNPLA3* and *TM6SF2* on non-alcoholic fatty liver disease (NAFLD) in a Chinese population. *Front Genet* 2016;7:140.
  - [30] **Li JZ, Huang Y, Karaman R, Ivanova PT, Brown HA, Roddy T, et al.** Chronic overexpression of *PNPLA3* in mouse liver causes hepatic steatosis. *J Clin Invest* 2012;122:4130–4144.
  - [31] **Smagris E, BasuRay S, Li J, Huang Y, Lai KM, Gromada J, et al.** *PNPLA3*148M knockin mice accumulate *PNPLA3* on lipid droplets and develop hepatic steatosis. *Hepatology* 2015;61:108–118.
  - [32] **Ehrhardt N, Doche ME, Chen S, Mao HZ, Walsh MT, Bedoya C, et al.** Hepatic *TM6SF2* overexpression affects cellular ApoB-trafficking, plasma lipid levels, hepatic steatosis and atherosclerosis. *Hum Mol Genet* 2017;26:2719–2731.
  - [33] **Lauridsen BK, Stender S, Kristensen TS, Kofoed KF, Kober L, Nordestgaard BG, et al.** Liver fat content, non-alcoholic fatty liver disease, and ischaemic heart disease: mendelian randomization and meta-analysis of 279 013 individuals. *Eur Heart J* 2018;39:385–393.
  - [34] **Wang N, Chen C, Zhao L, Chen Y, Han B, Xia F, et al.** Vitamin D and nonalcoholic fatty liver disease: bi-directional mendelian randomization analysis. *EBioMedicine* 2018;28:187–193.
  - [35] **Gorden A, Yang RZ, Yerges-Armstrong LM, Ryan KA, Speliotes E, Borecki IB, et al.** Genetic variation at NCAN locus is associated with inflammation and fibrosis in non-alcoholic fatty liver disease in morbid obesity. *Hum Hered* 2013;75:34–43.
  - [36] **Genomes Project C, Auton A, Brooks LD, Durbin RM, Garrison EP, Kang HM, et al.** A global reference for human genetic variation. *Nature* 2015;526:68–74.
  - [37] **Staiger D, Stock JH.** Instrumental variables regression with weak instruments. *Econometrica* 1997;65:557–586.
  - [38] **Burgess S, Butterworth A, Thompson SG.** Mendelian randomization analysis with multiple genetic variants using summarized data. *Genet Epidemiol* 2013;37:658–665.
  - [39] **Bowden J, Davey Smith G, Haycock PC, Burgess S.** Consistent estimation in mendelian randomization with some invalid instruments using a weighted median estimator. *Genet Epidemiol* 2016;40:304–314.
  - [40] **Bowden J, Davey Smith G, Burgess S.** Mendelian randomization with invalid instruments: effect estimation and bias detection through egger regression. *Int J Epidemiol* 2015;44:512–525.
  - [41] **Bowden J, Del Greco MF, Minelli C, Zhao Q, Lawlor DA, Sheehan NA, et al.** Improving the accuracy of two-sample summary-data Mendelian randomization: moving beyond the NOME assumption. *Int J Epidemiol* 2019;48:728–742.
  - [42] **Verbanck M, Chen CY, Neale B, Do R.** Detection of widespread horizontal pleiotropy in causal relationships inferred from Mendelian randomization between complex traits and diseases. *Nat Genet* 2018;50:693–698.
  - [43] **Yavorska OO, Burgess S.** MendelianRandomization: an R package for performing Mendelian randomization analyses using summarized data. *Int J Epidemiol* 2017;46:1734–1739.
  - [44] **Bowden J, Spiller W, Del Greco MF, Sheehan N, Thompson J, Minelli C, et al.** Improving the visualization, interpretation and analysis of two-sample summary data Mendelian randomization via the Radial plot and Radial regression. *Int J Epidemiol* 2018;47:2100.
  - [45] **Denk H, Abuja PM, Zatloukal K.** Animal models of NAFLD from the pathologist's point of view. *Biochim Biophys Acta Mol Basis Dis* 2019;1865:929–942.
  - [46] **Van Herck MA, Vonghia L, Francque SM.** Animal models of nonalcoholic fatty liver disease-A starter's guide. *Nutrients* 2017;9:1072.
  - [47] **Clapper JR, Hendricks MD, Gu G, Wittmer C, Dolman CS, Herich J, et al.** Diet-induced mouse model of fatty liver disease and nonalcoholic steatohepatitis reflecting clinical disease progression and methods of assessment. *Am J Physiol Gastrointest Liver Physiol* 2013;305:G483–G495.
  - [48] **Panasevich MR, Meers GM, Linden MA, Booth FW, Perfield 2nd JW, Fritsche KL, et al.** High-fat, high-fructose, high-cholesterol feeding causes severe NASH and cecal microbiota dysbiosis in juvenile Ossabaw swine. *Am J Physiol Endocrinol Metab* 2018;314:E78–E92.
  - [49] **Hemani G, Bowden J, Davey Smith G.** Evaluating the potential role of pleiotropy in Mendelian randomization studies. *Hum Mol Genet* 2018;27:R195–R208.
  - [50] **Ho KKY.** Diet-induced thermogenesis: fake friend or foe? *J Endocrinol* 2018;238:R185–R191.
  - [51] **Liao WH, Henneberg M, Langhans W.** Immunity-based evolutionary interpretation of diet-induced thermogenesis. *Cell Metab* 2016;23:971–979.
  - [52] **Kantartzis K, Peter A, Machicao F, Machann J, Wagner S, Konigsrainer I, et al.** Dissociation between fatty liver and insulin resistance in humans carrying a variant of the patatin-like phospholipase 3 gene. *Diabetes* 2009;58:2616–2623.
  - [53] **Peter A, Kovarova M, Nadalin S, Cermak T, Konigsrainer A, Machicao F, et al.** *PNPLA3* variant I148M is associated with altered hepatic lipid composition in humans. *Diabetologia* 2014;57:2103–2107.
  - [54] **Franko A, Merkel D, Kovarova M, Hoene M, Jaghutriz BA, Heni M, et al.** Dissociation of fatty liver and insulin resistance in I148M *PNPLA3* carriers: differences in diacylglycerol (DAG) FA18:1 lipid species as a possible explanation. *Nutrients* 2018;10:1314.
  - [55] **Palmer CN, Maglio C, Pirazzi C, Burza MA, Adiels M, Burch L, et al.** Paradoxical lower serum triglyceride levels and higher type 2 diabetes mellitus susceptibility in obese individuals with the *PNPLA3* 148M variant. *PLoS One* 2012;7:e39362.
  - [56] **Thomas NJ, Jones SE, Weedon MN, Shields BM, Oram RA, Hattersley AT.** Frequency and phenotype of type 1 diabetes in the first six decades of life: a cross-sectional, genetically stratified survival analysis from UK Biobank. *Lancet Diabetes Endocrinol* 2018;6:122–129.
  - [57] **Bao YK, Ma J, Ganesan VC, McGill JB.** Mistaken identity: missed diagnosis of type 1 diabetes in an older adult. *Med Res Arch* 2019;7:1962.
  - [58] **Radmard AR, Rahmiani MS, Abrishami A, Yoonessi A, Kooraki S, Dadgostar M, et al.** Assessment of abdominal fat distribution in non-alcoholic fatty liver disease by magnetic resonance imaging: a population-based study. *Arch Iran Med* 2016;19:693–699.
  - [59] **Pang Y, Kartsonaki C, Turnbull I, Guo Y, Chen Y, Clarke R, et al.** Adiposity in relation to risks of fatty liver, cirrhosis and liver cancer: a prospective study of 0.5 million Chinese adults. *Sci Rep* 2019;9:785.
  - [60] **Feldman A, Eder SK, Felder TK, Kedenko L, Paulweber B, Stadlmayr A, et al.** Clinical and metabolic characterization of lean Caucasian subjects with non-alcoholic fatty liver. *Am J Gastroenterol* 2017;112:102–110.
  - [61] **Lu FB, Hu ED, Xu LM, Chen L, Wu JL, Li H, et al.** The relationship between obesity and the severity of non-alcoholic fatty liver disease: systematic review and meta-analysis. *Expert Rev Gastroenterol Hepatol* 2018;12:491–502.
  - [62] **Tepper CG, Dang JHT, Stewart SL, Fang DM, Wong KA, Liu SY, et al.** High frequency of the *PNPLA3* rs738409 [G] single-nucleotide polymorphism in

- Hmong individuals as a potential basis for a predisposition to chronic liver disease. *Cancer* 2018;124(Suppl 7):1583–1589.
- [63] Pirazzi C, Adiels M, Burza MA, Mancina RM, Levin M, Stahlman M, et al. Patatin-like phospholipase domain-containing 3 (PNPLA3) I148M (rs738409) affects hepatic VLDL secretion in humans and in vitro. *J Hepatol* 2012;57:1276–1282.
- [64] Sadeghi M, Pourmoghaddas Z, Hekmatnia A, Sanei H, Tavakoli B, Tchernof A, et al. Abdominal fat distribution and serum lipids in patients with and without coronary heart disease. *Arch Iran Med* 2013;16:149–153.
- [65] Luo Y, Ma X, Shen Y, Hao Y, Hu Y, Xiao Y, et al. Positive relationship between serum low-density lipoprotein cholesterol levels and visceral fat in a Chinese nondiabetic population. *PLoS One* 2014;9:e112715.
- [66] Huang Y, He S, Li JZ, Seo YK, Osborne TF, Cohen JC, et al. A feed-forward loop amplifies nutritional regulation of *PNPLA3*. *Proc Natl Acad Sci U S A* 2010;107:7892–7897.
- [67] Liu W, Anstee QM, Wang X, Gawrieh S, Gamazon ER, Athinarayanan S, et al. Transcriptional regulation of *PNPLA3* and its impact on susceptibility to nonalcoholic fatty liver disease (NAFLD) in humans. *Aging (Albany NY)* 2016;9:26–40.
- [68] Wang Y, Kory N, BasuRay S, Cohen JC, Hobbs HH. PNPLA3, CGI-58, and inhibition of hepatic triglyceride hydrolysis in mice. *Hepatology* 2019;69:2427–2441.
- [69] Lee YH, Cho Y, Lee BW, Park CY, Lee DH, Cha BS, et al. Nonalcoholic fatty liver disease in diabetes. Part I: epidemiology and diagnosis. *Diabetes Metab J* 2019;43:31–45.
- [70] Denkmayr L, Feldman A, Stechemesser L, Eder SK, Zandanel S, Schranz M, et al. Lean patients with non-alcoholic fatty liver disease have a severe histological phenotype similar to obese patients. *J Clin Med* 2018;7:562.
- [71] Colombo M, Pelusi S. Towards precision medicine in nonalcoholic fatty liver disease with PNPLA3 as a therapeutic Target. *Gastroenterology* 2019;157:1156–1157.
- [72] Linden D, Ahnmark A, Pingitore P, Ciociola E, Ahlstedt I, Andreasson AC, et al. *PNPLA3* silencing with antisense oligonucleotides ameliorates nonalcoholic steatohepatitis and fibrosis in PNPLA3 I148M knock-in mice. *Mol Metab* 2019;22:49–61.